

Observation of a Coherence Length Effect in Exclusive ρ^0 Electroproduction

K. Ackerstaff,⁵ A. Airapetian,³⁴ N. Akopov,³⁴ I. Akushevich,⁶ M. Amarian,^{34,29,25} E. C. Aschenauer,^{6,13,14,25} H. Avakian,¹⁰ R. Avakian,³⁴ A. Avetissian,³⁴ B. Bains,¹⁵ S. Barrow,²⁷ C. Baumgarten,²³ M. Beckmann,¹² St. Belostotski,²⁸ J. E. Belz,^{4,30,31} Th. Benisch,⁸ S. Bernreuther,⁸ N. Bianchi,¹⁰ S. Blanchard,²⁴ J. Blouw,²⁵ H. Böttcher,⁶ A. Borissov,^{6,14} J. Brack,⁴ S. Brauksiepe,¹² B. Braun,^{8,23} B. Bray,³ St. Brons,⁶ W. Brückner,¹⁴ A. Brüll,¹⁴ E. E. W. Bruins,²⁰ H. J. Bulten,^{18,25,33} R. V. Cadman,¹⁵ G. P. Capitani,¹⁰ P. Carter,³ P. Chumney,²⁴ E. Cisbani,²⁹ G. R. Court,¹⁷ P. F. Dalpiaz,⁹ P. P. J. Delheij,³¹ E. De Sanctis,¹⁰ D. De Schepper,²⁰ E. Devitsin,²² P. K. A. de Witt Huberts,²⁵ P. Di Nezza,¹⁰ M. Düren,⁸ A. Dvoredsky,³ G. Elbakian,³⁴ J. Ely,⁴ J. Emerson,^{30,31} A. Fantoni,¹⁰ A. Fechtchenko,⁷ M. Ferstl,⁸ D. Fick,¹⁹ K. Fiedler,⁸ B. W. Filippone,³ H. Fischer,¹² H. T. Fortune,²⁷ B. Fox,⁴ S. Frabetti,⁹ J. Franz,¹² S. Frullani,²⁹ M.-A. Funk,⁵ N. D. Gagunashvili,⁷ P. Galumian,¹ H. Gao,^{2,15,20} Y. Gärber,⁶ F. Garibaldi,²⁹ G. Gavrillov,²⁸ P. Geiger,¹⁴ V. Gharibyan,³⁴ V. Giordjian,¹⁰ A. Golendukhin,^{19,34} G. Graw,²³ O. Grebeniouk,²⁸ P. W. Green,^{1,31} L. G. Greeniaus,^{1,31} C. Grosshauser,⁸ M. G. Guidal,²⁵ A. Gute,⁸ V. Gyurjyan,¹⁰ J. P. Haas,²⁴ W. Haeberli,¹⁸ J.-O. Hansen,² D. Hasch,⁶ O. Häusser,^{30,31,*} F. H. Heinsius,¹² R. S. Henderson,³¹ Th. Henkes,²⁵ M. Henoeh,⁸ R. Hertenberger,²³ Y. Holler,⁵ R. J. Holt,¹⁵ W. Hoprich,¹⁴ H. Ihssen,^{5,25} M. Iodice,²⁹ A. Izotov,²⁸ H. E. Jackson,² A. Jgoun,²⁸ C. Jones,² R. Kaiser,^{30,31} E. Kinney,⁴ M. Kirsch,⁸ A. Kisselev,²⁸ P. Kitching,¹ H. Kobayashi,³² N. Koch,¹⁹ K. Königsmann,¹² M. Kolstein,²⁵ H. Kolster,²³ V. Korotkov,⁶ W. Korsch,^{3,16} V. Kozlov,²² L. H. Kramer,^{20,11} B. Krause,⁶ V. G. Krivokhijine,⁷ M. Kückes,^{30,31} F. Kümmell,¹² G. Kyle,²⁴ W. Lachnit,⁸ W. Lorenzon,^{27,21} A. Lung,³ N. C. R. Makins,^{2,15} F. K. Martens,¹ J. W. Martin,²⁰ F. Masoli,⁹ A. Mateos,²⁰ M. McAndrew,¹⁷ K. McIlhany,³ R. D. McKeown,³ F. Meissner,⁶ F. Menden,^{12,31} D. Mercer,⁴ A. Metz,²³ N. Meyners,⁵ O. Mikloukho,²⁸ C. A. Miller,^{1,31} M. A. Miller,¹⁵ R. G. Milner,²⁰ V. Mitsyn,⁷ A. Most,^{15,21} R. Mozzetti,¹⁰ V. Muccifora,¹⁰ A. Nagaitsev,⁷ Y. Naryshkin,²⁸ A. M. Nathan,¹⁵ F. Neunreither,⁸ M. Niczyporuk,²⁰ W.-D. Nowak,⁶ M. Nupieri,¹⁰ P. Oelwein,¹⁴ H. Ogami,³² T. G. O'Neill,² R. Openshaw,³¹ J. Ouyang,³¹ B. R. Owen,¹⁵ V. Papavassiliou,²⁴ S. F. Pate,^{20,24} M. Pitt,³ H. R. Poolman,²⁵ S. Potashov,²² D. H. Potterveld,² B. Povh,¹⁴ G. Rakness,⁴ A. Reali,⁹ R. Redwine,²⁰ A. R. Reolon,¹⁰ R. Ristinen,⁴ K. Rith,⁸ H. Roloff,⁶ G. Röper,⁵ P. Rossi,¹⁰ S. Rudnitsky,²⁷ M. Ruh,¹² D. Ryckbosch,¹³ Y. Sakemi,³² I. Savin,⁷ C. Scarlett,²¹ F. Schmidt,⁸ H. Schmitt,¹² G. Schnell,²⁴ K. P. Schüller,⁵ A. Schwind,⁶ J. Seibert,¹² T.-A. Shibata,³² T. Shin,²⁰ V. Shutov,⁷ C. Simani,⁹ A. Simon,^{12,24} K. Sinram,⁵ P. Slavich,^{9,10} J. Sowinski,¹⁴ M. Spengos,^{27,5} E. Steffens,⁸ J. Stenger,⁸ J. Stewart,¹⁷ F. Stock,^{14,8} U. Stoesslein,⁶ M. Sutter,²⁰ H. Tallini,¹⁷ S. Taroian,³⁴ A. Terkulov,²² D. M. Thiessen,^{30,31} E. Thomas,¹⁰ B. Tipton,²⁰ A. Trudel,^{30,31} M. Tytgat,¹³ G. M. Urciuoli,²⁹ J. J. van Hunen,²⁵ R. van de Vyver,¹³ J. F. J. van den Brand,^{18,25,33} G. van der Steenhoven,²⁵ M. C. Vetterli,^{30,31} V. Vikhrov,²⁸ M. Vinciter,³¹ J. Visser,²⁵ E. Volk,¹⁴ W. Wander,⁸ T. P. Welch,²⁶ S. E. Williamson,¹⁵ T. Wise,¹⁸ T. Wölfel,⁸ K. Woller,⁵ S. Yoneyama,³² K. Zapfe-Düren,⁵ H. Zohrabian,³⁴ and R. Zurmühle²⁷

(HERMES Collaboration)

¹Department of Physics, University of Alberta, Edmonton, Alberta T6G 2J1, Canada

²Physics Division, Argonne National Laboratory, Argonne, Illinois 60439-4843

³W. K. Kellogg Radiation Lab, California Institute of Technology, Pasadena, California 91125

⁴Nuclear Physics Laboratory, University of Colorado, Boulder, Colorado 80309-0446

⁵DESY, Deutsches Elektronen Synchrotron, D-22603 Hamburg, Germany

¹DESY Zeuthen, D-15738 Zeuthen, Germany

⁷Joint Institute for Nuclear Research, 141980 Dubna, Russia

⁸Physikalisches Institut, Universität Erlangen-Nürnberg, D-91058 Erlangen, Germany

⁹Dipartimento di Fisica, Università di Ferrara, I-44100 Ferrara, Italy

¹⁰Istituto Nazionale di Fisica Nucleare, Laboratori Nazionali di Frascati, I-00044 Frascati, Italy

¹¹Department of Physics, Florida International University, Miami, Florida 33199

¹²Fakultät für Physik, Universität Freiburg, D-79104 Freiburg, Germany

¹³Department of Subatomic and Radiation Physics, University of Gent, B-9000 Gent, Belgium

¹⁴Max-Planck-Institut für Kernphysik, D-69029 Heidelberg, Germany

¹⁵Department of Physics, University of Illinois, Urbana, Illinois 61801

¹⁶Department of Physics and Astronomy, University of Kentucky, Lexington, Kentucky 40506

¹⁷Physics Department, University of Liverpool, Liverpool L69 7ZE, United Kingdom

¹⁸Department of Physics, University of Wisconsin—Madison, Madison, Wisconsin 53706

¹⁹Physikalisches Institut, Philipps-Universität Marburg, D-35037 Marburg, Germany

²⁰Laboratory for Nuclear Science, Massachusetts Institute of Technology, Cambridge, Massachusetts 02139

²¹Randall Laboratory of Physics, University of Michigan, Ann Arbor, Michigan 48109-1120

²²Lebedev Physical Institut, 117924 Moscow, Russia

²³Sektion Physik, Universität München, D-85748 Garching, Germany

²⁴Department of Physics, New Mexico State University, Las Cruces, New Mexico 88003

²⁵Nationaal Instituut voor Kernfysica en Hoge-Energiefysica (NIKHEF), NL-1009 DB Amsterdam, The Netherlands

²⁶Physics Department, Oregon State University, Corvallis, Oregon 97331

²⁷Department of Physics and Astronomy, University of Pennsylvania, Philadelphia, Pennsylvania 19104-6396

²⁸Petersburg Nuclear Physics Institute, St. Petersburg, 188350 Russia

²⁹Istituto Nazionale di Fisica Nucleare, Sezione Sanità and Physics Laboratory, Istituto Superiore di Sanità, I-00161 Roma, Italy

³⁰Department of Physics, Simon Fraser University, Burnaby, British Columbia V5A 1S6, Canada

³¹TRIUMF, Vancouver, British Columbia V6T 2A3, Canada

³²Department of Physics, Tokyo Institute of Technology, Tokyo 152-8551, Japan

³³Department of Physics and Astronomy, Vrije Universiteit, NL-1081 HV Amsterdam, The Netherlands

³⁴Yerevan Physics Institute, 375036, Yerevan, Armenia

(Received 5 November 1998)

Exclusive incoherent electroproduction of the $\rho^0(770)$ meson from ^1H , ^2H , ^3He , and ^{14}N targets has been studied by the HERMES experiment at squared four-momentum transfer $Q^2 > 0.4 \text{ GeV}^2$ and positron energy loss ν from 9 to 20 GeV. The ratio of the ^{14}N to ^1H cross sections per nucleon, known as the nuclear transparency, was found to decrease with increasing coherence length of quark-antiquark fluctuations of the virtual photon. The data provide clear evidence of the interaction of the quark-antiquark fluctuations with the nuclear medium. [S0031-9007(99)08858-4]

PACS numbers: 13.60.Le, 14.40.Cs, 24.85.+p, 25.30.Rw

The space-time evolution of a virtual quantum state, such as a quark-antiquark ($q\bar{q}$) fluctuation of a photon, can be probed by studying its propagation through a perturbing medium. The unperturbed virtual state can travel a distance l_c , known as the “coherence length,” in the laboratory frame during its lifetime. The interactions between the state and the medium can be studied at different values of l_c by varying the kinematics at which the state is produced. In this Letter, interactions of a $q\bar{q}$ fluctuation with the nuclear medium are studied by measuring the nuclear dependence of the exclusive ρ^0 electroproduction cross section.

Studies of the hadronic ($q\bar{q}$) structure of high-energy photons started with groundwork by Yang and Mills, Sakurai, Gell-Mann and Zachariasen, and Berman and Drell in the early 1960s [1]. The hadronic structure arises from fluctuations of the (real or virtual) photon to short-lived quark-antiquark states of mass $M_{q\bar{q}}$ and propagation distance $l_c = 2\nu/(Q^2 + M_{q\bar{q}}^2)$ [2–4], where $-Q^2$ and ν are the squared mass and laboratory-frame energy of the photon (adopting units where $\hbar = c = 1$). The $q\bar{q}$ fluctuations are assumed to dominate many photon-induced reactions in the laboratory frame [2]. For example, in exclusive production of the ρ^0 meson, a $q\bar{q}$ pair is scattered onto the physical ρ^0 mass shell by a diffractive interaction with the target [2–5].

In nuclear targets, photon-induced reactions can be affected by the initial state interactions (ISI) of the $q\bar{q}$ states with the nuclear medium. The ISI are maximized when l_c is large compared to the nuclear radius R_A , and the photon converts to the $q\bar{q}$ pair before entering the nucleus [2–4]. The hadronic ISI vanish in the limit $l_c \ll$

R_A of negligible $q\bar{q}$ interaction path. The dependence of the ISI on l_c can be measured explicitly in exclusive ρ^0 production experiments, where a single mass—namely, the ρ^0 mass—dominates $M_{q\bar{q}}$ and l_c [2–4]. Largely because of limited coverage in l_c , previous experiments have not yet seen the expected l_c dependence [2,6].

In exclusive reactions a specific final state is produced without additional particles, for example, $eN \rightarrow e\rho^0 N$ (here N is a nucleon). The effect of the nuclear medium on the particles in the initial and final states of such reactions can be characterized by the nuclear transparency T_A . It is defined as the ratio of the measured cross section to that expected in the absence of these initial and final state interactions (FSI). If the ISI and FSI amplitudes factorize from the exclusive scattering amplitude, then T_A is the probability that no significant ISI or FSI occur. The transparency has been used to study the space-time dynamics of several exclusive reactions [2,6–9]. This paper reports measurements of the nuclear transparency for exclusive incoherent ρ^0 electroproduction on ^2H , ^3He , and ^{14}N targets at $Q^2 > 0.4 \text{ GeV}^2$, $9 < \nu < 20 \text{ GeV}$, and $0.6 \leq l_c < 8 \text{ fm}$. The data provide an explicit demonstration that the interactions of the photon with the nuclear medium depend on the propagation distance l_c of the $q\bar{q}$ pair.

The data were obtained during the 1995–1997 running periods of the HERMES experiment in the 27.5 GeV HERA positron storage ring at DESY. Stored currents ranged from 5 to 40 mA. Integrated luminosities of 93.7, 83.6, 100.3, and 40.5 pb^{-1} were collected on ^1H , ^2H , ^3He , and ^{14}N internal gas targets, respectively. The respective time average target thicknesses were 0.1×10^{15} , 1.6×10^{15} , 0.8×10^{15} , and 1×10^{15} nucleons/cm².

The thicknesses were varied from roughly half to roughly 10 times these values, depending on how much the HERMES internal target was allowed to limit the HERA beam lifetime. The scattered e^+ and the $\pi^+\pi^-$ pair from the ρ^0 decay ($\approx 100\%$ branching ratio) were detected in the HERMES forward spectrometer [10].

The ρ^0 production sample was extracted from events with exactly three tracks: a scattered positron and two oppositely charged hadrons. The relevant four-momenta are the following: k (k') of the incident (scattered) positron, $q \equiv k - k'$ of the virtual photon, P of the struck nucleon, P_{h^+} and P_{h^-} of the detected hadrons, $\nu \equiv P_{h^+} + P_{h^-}$ of the ρ^0 candidate, and $P_Y \equiv P + q - \nu$ of the undetected final state Y . The relevant Lorentz invariants are the following: $Q^2 = -q^2 > 0$; $\nu = qP/M$ (here M is the proton mass); and exclusivity measure $\Delta E = (P_Y^2 - M^2)/2M$; the invariant mass $M_{\pi\pi} = \sqrt{\nu^2}$ assuming the detected hadrons are pions; the squared four-momentum transfer $t = (q - \nu)^2$ to the target; the maximum value t_0 of t for fixed ν , Q^2 , P_Y^2 , and $M_{\pi\pi}$; and the above-threshold momentum transfer $t' = t - t_0 < 0$.

For nuclear targets, the diffractive interaction with the target can occur incoherently from individual nucleons or coherently from the nucleus as a whole. The incoherent exclusive ρ^0 production signal was extracted in the kinematic region $t'_i < -t' < 0.4 \text{ GeV}^2$, $-2 < \Delta E < 0.6 \text{ GeV}$, $0.6 < M_{\pi\pi} < 1 \text{ GeV}$, and $9 < \nu < 20 \text{ GeV}$. The lower $-t'$ limit, t'_i , is chosen separately for each target and l_c bin to maximize statistics while keeping small the contribution from coherent scattering; t'_i is 0.03 to 0.06 GeV^2 for ^2H , 0.03 to 0.14 GeV^2 for ^3He , and 0.05 to 0.09 GeV^2 for ^{14}N .

The distribution of the selected events in ΔE is shown for all targets in Fig. 1a. Exclusive $eN \rightarrow eh^+h^-N$ events, where the undetected final state consists of a nucleon recoiling without excitation, occur at $\Delta E = 0$. *Nonexclusive* events that involve the production of additional, undetected particles appear at larger ΔE . The events with $\Delta E \gtrsim 3 \text{ GeV}$ are predominantly due to deep inelastic scattering (DIS). The ΔE dependence of DIS events is measured at $0.7 < -t' < 5 \text{ GeV}^2$ where the diffractive exclusive signal is negligible (see histogram in Fig. 1a). The DIS background below the exclusive peak is subtracted for each target and kinematic bin separately, assuming the shape of the background is independent of t' and normalizing to the number of events measured at $t'_i < -t' < 0.4 \text{ GeV}^2$ and $\Delta E > 3 \text{ GeV}$. The difference at $\Delta E \sim 2 \text{ GeV}$ between the two distributions shown in Fig. 1a is due mainly to the radiative tail of the exclusive peak and to ρ^0 production events where the diffractive interaction excites the nucleon. Except for small kinematic shifts, these processes do not affect the propagation of the virtual photon or outgoing ρ^0 through the nuclear medium.

The exclusive $M_{\pi\pi}$ distribution, shown in Fig. 1b, is dominated by resonant production of the $\rho^0(770)$, with

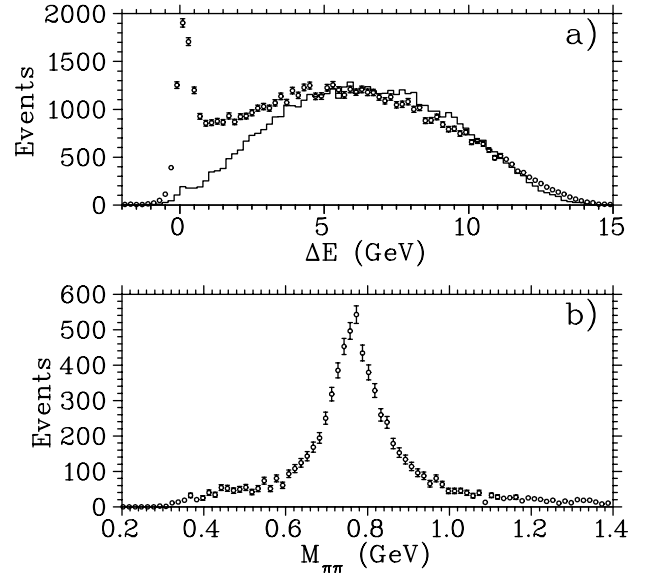


FIG. 1. (a) Measured events as a function of exclusivity variable ΔE for the ^1H , ^2H , ^3He , and ^{14}N data passing the experimental cuts; the distribution is shown for $0.1 < -t' < 0.4 \text{ GeV}^2$ (open circles) and for $0.7 < -t' < 5 \text{ GeV}^2$ (histogram, scaled to the same total counts at $\Delta E > 3 \text{ GeV}$). (b) Invariant mass distribution for the exclusive events at $0.1 < -t' < 0.4 \text{ GeV}^2$.

small interfering contributions from exclusive production of nonresonant $\pi^+\pi^-$ pairs and of the $\omega(782)$ resonance (in its 2% decay branch to $\pi^+\pi^-$ [11]). Background from the two-kaon decay of exclusively produced $\phi(1020)$ mesons, which would appear at $M_{\pi\pi} < 0.5 \text{ GeV}$, is eliminated by requiring that the two-kaon invariant mass be greater than 1.04 GeV .

The exclusive $-t'$ distributions for the ^1H , ^2H , ^3He , and ^{14}N nuclei are shown in Fig. 2. The data exhibit the rapid falloff expected for a diffractive process. To isolate incoherent scattering, the data are fit to a shape giving the sum of incoherent and coherent contributions, $b_N e^{b_N t'} + f_A b_A e^{b_A t'}$ (solid curves). Here f_A is the ratio of coherent to incoherent total counts and $e^{b_N t'}$ ($e^{b_A t'}$) represents the product of the ρ^0 and struck nucleon (nucleus) elastic form factors, squared [12]. The incoherent slope parameter b_N for each nucleus (measured to an accuracy of about 0.5 GeV^{-2}) is consistent with the hydrogen value $b_N = (6.82 \pm 0.15) \text{ GeV}^{-2}$. The coherent slope parameters $b_{^2\text{H}} = (33.3 \pm 9.8) \text{ GeV}^{-2}$, $b_{^3\text{He}} = (32.5 \pm 5.7) \text{ GeV}^{-2}$, and $b_{^{14}\text{N}} = (57.2 \pm 3.3) \text{ GeV}^{-2}$ are consistent with the values predicted by the relationship $b_A \approx R_A^2/3$ [12] and the measured electromagnetic rms radii $R_{^2\text{H}} = 2.1 \text{ fm}$, $R_{^3\text{He}} = 1.9 \text{ fm}$, and $R_{^{14}\text{N}} = 2.5 \text{ fm}$ [13].

In the absence of ISI and FSI, the cross section σ_A for incoherent ρ^0 production from a nucleus with A nucleons would be $A\sigma_H$ (assuming the expected isospin symmetry $\sigma_n = \sigma_H$ [2], where n and H refer to the neutron and ^1H). The nuclear transparency is therefore $T_A \equiv \sigma_A/(A\sigma_H) = N_A L_H/(A N_H L_A)$, where the second equality follows from

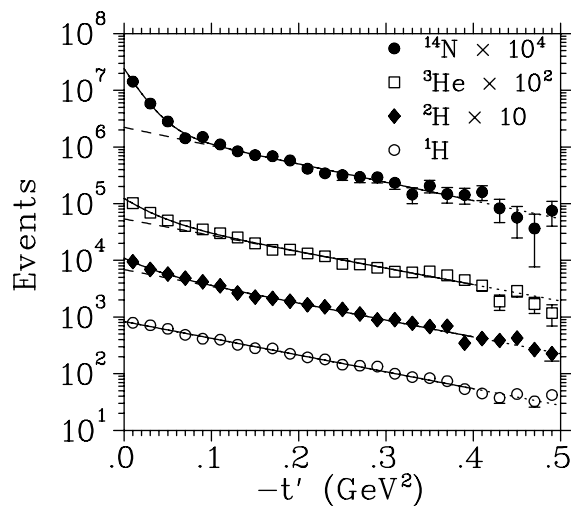


FIG. 2. Distribution of momentum transfer t' for exclusive ρ^0 production from ^1H , ^2H , ^3He , and ^{14}N targets. The solid curves are fit to the shape $b_N e^{b_N t'} + f_A b_A e^{b_A t'}$, the dotted lines are extrapolations beyond the fit interval $-t' < 0.4 \text{ GeV}^2$, and the dashed lines are the inferred incoherent contributions.

the A independence of the experimental acceptance. Here $N_{A,H}$ is the number of incoherent events in the range $t'_i < -t' < 0.4 \text{ GeV}^2$; N_A is corrected for the coherent contribution using the t' fit for each l_c bin (t'_i is chosen so that the correction factor is less than 1.05 with an uncertainty of less than 4%). The integral $L_{A,H}$ of the effective luminosity is determined from the number of inclusive DIS positrons and the published nuclear DIS structure functions [14], with a correction for the efficiency (≥ 0.8) for tracking the h^+h^- pair.

The systematic uncertainties are separated into l_c -independent and l_c -dependent contributions. The respective contributions from possible differences in the spectrometer performance for the nuclear and ^1H data are estimated to be no more than 5.2% and 4% for any nucleus by studying the time dependence of $N_{A,H}/L_{A,H}$ and other normalized yields. The respective contributions from the treatment of the nonexclusive background is no more than 3.5% and 1.6%, based on the dependence of T_A on ΔE . For the incoherent events selected in the analysis and target thicknesses of less than 10^{-8} radiation lengths, internal and external radiative effects are determined to cancel to high precision ($< 0.3\%$) in the nuclear ratio. The resulting kinematics-independent systematic uncertainty in the overall normalization of $T_{^2\text{H}}$, $T_{^3\text{He}}$, or $T_{^{14}\text{N}}$ is 2.7%, 5.5%, or 5.9%, respectively. The kinematics-dependent point-to-point systematic uncertainty includes an additional contribution from the fit uncertainty in the coherent contribution, and is never larger than 5.7%. The T_A results are unchanged at the 3% level (and the systematic uncertainties are essentially unchanged) if the nonexclusive background is not subtracted.

The nuclear transparencies for ^2H (filled diamond), ^3He (open square), and ^{14}N (filled circle) are shown as functions of the coherence length l_c in Fig. 3. Within uncertainties the ^2H and ^3He transparencies are independent of l_c : $T_{^2\text{H}} = 0.970 \pm 0.024 \text{ (stat)} \pm 0.040 \text{ (syst)}$ and $T_{^3\text{He}} = 0.862 \pm 0.042 \pm 0.061$. The consistency of the deuterium transparency with unity suggests that $\sigma_n \approx \sigma_H$ and that the ISI and FSI are small in ^2H . The average ^3He transparency is 1.9 standard deviations below unity.

The nitrogen transparency exhibits the decrease expected from the onset of hadronic ISI as l_c increases. The decrease from 0.681 ± 0.060 at $l_c < 2 \text{ fm}$ to 0.401 ± 0.054 at $l_c > 3.6 \text{ fm}$ has a 3.5 standard deviation statistical significance. These errors comprise statistical and l_c -dependent systematic uncertainties added in quadrature; the normalization systematic uncertainty is not included, because it does not influence the l_c dependence. In the absence of ISI variations, the transparency would exhibit

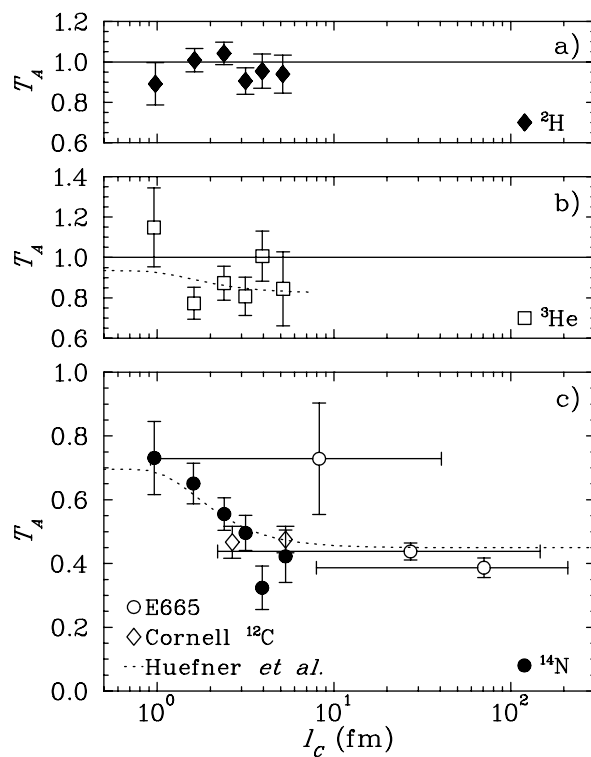


FIG. 3. Nuclear transparency T_A as a function of l_c for (a) ^2H (filled diamond), (b) ^3He (open square), and (c) ^{14}N (filled circle) targets. The error bars include statistical and point-to-point systematic uncertainties added in quadrature. The respective 2.5%, 5.5%, and 5.9% systematic uncertainties in the overall normalizations of $T_{^2\text{H}}$, $T_{^3\text{He}}$, and $T_{^{14}\text{N}}$ are not shown, since they do not influence the significance of the l_c dependences. Panel (c) includes comparisons with previous experiments with photon (open diamonds) [6] and muon (open circle) [8] beams. Because of the acceptance for $20 < \nu \leq 370 \text{ GeV}$, the three Q^2 bins measured by [8] correspond to broad ranges in l_c (horizontal error bars). The dashed curves are the Glauber calculation of Hüfner *et al.* for ^3He and ^{14}N [3].

a small ($<3\%$) increase with l_c due to the known [2] energy dependence of the $\rho^0 N$ cross section.

Figure 3c also shows the transparency to incoherent ρ^0 production measured at Cornell with 4 and 8 GeV photons [6] and by the E655 collaboration at FNAL with 470 GeV muons [8]. These results are consistent with the present data but give no indication of a variation with l_c . The E665 $T_{^{14}\text{N}}$ values are inferred from the published A dependence [8]. The E665 value for $T_{^{14}\text{N}}$ at $l_c \sim 8$ fm was measured at $\nu \gtrsim 100$ GeV and $Q^2 > 3$ GeV² [8], and may therefore be influenced by color transparency. Color transparency implies that at high Q^2 and ν the $q\bar{q}$ pair (and the subsequent ρ^0) is produced and propagates in a noninteracting configuration of reduced transverse size, resulting in $T_A \rightarrow 1$ [2,5,15,16]. For this reason data collected by the NMC collaboration with a muon beam at $40 < \nu < 180$ GeV and $Q^2 > 2$ GeV² [9] are not included in Fig. 3c.

The $T_{^{14}\text{N}}$ and $T_{^3\text{He}}$ data are consistent with a recent prediction (dashed curves in Fig. 3) of the coherence length effect [3], although the statistics for $T_{^3\text{He}}$ are not sufficient to demonstrate the l_c variation. The prediction uses Glauber multiple-scattering theory [17], where the total ρ^0 production amplitude is the sum of the amplitudes from each nucleon, modified by elastic and inelastic rescattering of the outgoing ρ^0 on the other nucleons. In this model, the $q\bar{q}$ fluctuation from which the ρ^0 originates is found to interact with the nuclear medium like a ρ^0 [3]. The strength of the ρ^0 and $q\bar{q}$ interactions govern the transparency at small l_c and its l_c dependence, respectively. The consistency of the model with the data therefore suggests that when l_c is large, the $q\bar{q}$ ISI are approximately as strong as the ρ^0 FSI. For the ν values of the present measurement, color transparency is expected to produce little deviation from the Glauber prediction [3,16].

The data support the hypothesis [2,18] that absorption of the photon's $q\bar{q}$ component contributes to the shadowing observed in real and virtual photon nuclear cross sections. Shadowing denotes that the cross sections grow more slowly than linearly in A . It is observed for inclusive DIS at small Bjorken $x = Q^2/2M\nu$ and for elastic and inclusive real photon scattering at high energies.

In summary, the transparency of the ^2H , ^3He , and ^{14}N nuclei to exclusive incoherent ρ^0 electroproduction was measured by the HERMES experiment as a function of the coherence length of $q\bar{q}$ fluctuations of the virtual photon. The measured transparencies agree well with previous data and with a prediction using the standard treatment of high-energy initial and final state interactions. The transparency of the nitrogen nucleus exhibits a significant decrease with l_c , which is attributed to initial state interactions of the $q\bar{q}$ fluctuation from which the ρ^0 originates.

We gratefully acknowledge the DESY management for its support and the DESY staff and the staffs of the

collaborating institutions. We also thank B.Z. Kopeliovich, J. Nemchik, M. Strikman, and especially D.F. Geesaman for helpful discussions. This work was supported by the FWO-Flanders, Belgium; the Natural Sciences and Engineering Research Council of Canada; the INTAS and TMR network contributions from the European Community; the German Bundesministerium für Bildung, Wissenschaft, Forschung und Technologie; the Deutscher Akademischer Austauschdienst (DAAD); the Italian Istituto Nazionale di Fisica Nucleare (INFN); Monbusho, JSPS, and Toray Science Foundation of Japan; the Dutch Foundation for Fundamental Onderzoek der Materie (FOM); the U.K. Particle Physics and Astronomy Research Council; and the U.S. Department of Energy and National Science Foundation.

*Deceased.

- [1] C. N. Yang and R. L. Mills, Phys. Rev. **96**, 191 (1954); J. J. Sakurai, Ann. Phys. (N.Y.) **11**, 1 (1960); M. Gell-Mann and F. Zachariasen, Phys. Rev. **124**, 953 (1961); S. M. Berman and S. D. Drell, Phys. Rev. **133**, B791 (1964).
- [2] T. H. Bauer *et al.*, Rev. Mod. Phys. **50**, 261 (1978), and references therein.
- [3] J. Hüfner *et al.*, Phys. Lett. B **383**, 362 (1996); B. Z. Kopeliovich and J. Nemchik (private communication).
- [4] K. Gottfried and D. R. Yennie, Phys. Rev. **182**, 1595 (1969).
- [5] S. J. Brodsky *et al.*, Phys. Rev. D **50**, 3134 (1994).
- [6] G. N. McClellan *et al.*, Phys. Rev. Lett. **23**, 554 (1969).
- [7] A. S. Carroll *et al.*, Phys. Rev. Lett. **61**, 1698 (1988); T. G. O'Neill *et al.*, Phys. Lett. B **351**, 87 (1995).
- [8] M. R. Adams *et al.*, Phys. Rev. Lett. **74**, 1525 (1995).
- [9] M. Arneodo *et al.*, Nucl. Phys. **B429**, 503 (1994).
- [10] K. Ackerstaff *et al.*, Phys. Lett. B **404**, 383 (1997); K. Ackerstaff *et al.*, Nucl. Instrum. Methods Phys. Res., Sect. A **417**, 230 (1998).
- [11] Particle Data Group, C. Caso *et al.*, Eur. Phys. J. C **3**, 1 (1998).
- [12] B. Povh and J. Hüfner, Phys. Rev. Lett. **58**, 1612 (1987).
- [13] H. de Vries *et al.*, At. Data Nucl. Data Tables **36**, 495 (1987).
- [14] P. Amaudruz *et al.*, Nucl. Phys. **B441**, 3 (1995).
- [15] S. J. Brodsky and A. H. Mueller, Phys. Lett. B **206**, 685 (1988); L. L. Frankfurt *et al.*, Annu. Rev. Nucl. Part. Sci. **45**, 501 (1994); B. Z. Kopeliovich *et al.*, Phys. Lett. B **324**, 469 (1994); P. Jain *et al.*, Phys. Rep. **271**, 67 (1996); O. Benhar *et al.*, J. Exp. Theor. Phys. **84**, 421 (1997).
- [16] J. Hüfner and B. Z. Kopeliovich, Phys. Lett. B **403**, 128 (1997).
- [17] R. J. Glauber, in *Lectures in Theoretical Physics*, edited by W. E. Brittin and L. G. Duham (Intersciences, New York, 1959), Vol. 1.
- [18] B. Badelek and J. Kwiciński, Rev. Mod. Phys. **68**, 445 (1996), and references therein; G. Piller and W. Weise, Phys. Rev. C **42**, R1834 (1990).